P₄ Activation

DOI: 10.1002/ange.200601048

A Snapshot of P_4 Tetrahedron Opening: Rh- and Ir-Mediated Activation of White Phosphorus**

Dmitry Yakhvarov, Pierluigi Barbaro, Luca Gonsalvi, Sonia Mañas Carpio, Stefano Midollini,* Annabella Orlandini, Maurizio Peruzzini,* Oleg Sinyashin, and Fabrizio Zanobini*

The reactivity of white phosphorus with transition metals is characterized by a vast diversity of bonding situations which result in various $\{P_x\}$ units that range from single phosphido atoms to high-nuclearity polyphosphorus ligands.[1] When the tetraphosphorus array is preserved, different topologies are observed in which the P_4 molecule either remains intact and behaves as a monohapto[2] or dihapto ligand,[2c,3] or is activated by the opening of one or more edges to generate acyclic P_4 chains.[1a–d] These ligands reach their thermodynamic minima either by bridging two metal moieties[4] or by undergoing electrophilic or nucleophilic attack from ancillary ligands to form new P–H, P–C, or P–P bonds,[5] as exemplified by the recently reported dithallium salt of $Ar_2P_4^{2-}$ (**1**, $Ar = C_6H_3$-2,6-(C_6H_3-2,6-iPr$_2$)$_2$)[5c] and the unique cobalt complex $[Co(Ph_2PCH_2PPh_2PPPPPh_2PCH_2PPh_2)]BF_4$ (**2**-BF_4)

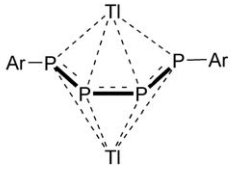

1, Ar = C_6H_3-2,6-(C_6H_3-2,6-iPr$_2$)$_2$

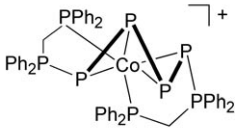

2

[*] Dr. D. Yakhvarov, Prof. O. Sinyashin
A. E. Arbuzov Institute of Organic and Physical Chemistry
Russian Academy of Sciences
Arbuzov str. 8, 420088 Kazan (Russian Federation)
Fax: (+7) 8432-732-253
E-mail: yakhvar@iopc.knc.ru
Dr. P. Barbaro, Dr. L. Gonsalvi, Dr. S. Mañas Carpio, Dr. S. Midollini, Dr. A. Orlandini, Dr. M. Peruzzini, Dipl. Chem. F. Zanobini
Istituto di Chimica dei Composti Organometallici
ICCOM CNR
Via Madonna del Piano, 10, 50019 Sesto Fiorentino (Italy)
Fax (+39) 055-5225-203
E-mail: stefano.midollini@iccom.cnr.it
mperuzzini@iccom.cnr.it

[**] The stay of D.Y. in Florence was supported by the INTAS YS fellowship program 2003 (Fellowship Ref. Nr. 03-55-2050). S.M.C. thanks the "Ministerio de Ciencia y Tecnologia" (Spain) for a postdoctoral grant. Thanks are due to Thermphos Int. (Vlissingen, Netherlands) for a generous loan of white phosphorus, to the NMR service of "FIRENZE HYDROLAB", a project sponsored by Ente Cassa di Risparmio di Firenze, and to Dr. A. Raffaelli (ICCOM CNR, Pisa) for running the ESI-MS spectrum of **5**-OTf.

Supporting information for this article is available on the WWW under http://www.angewandte.org or from the author.

which was prepared in our group more than two decades ago.[6] The mechanism of formation of the cobalt(I)-coordinated 1,4-disubstituted zigzag tetraphosphabutadiene P_6 chain in **2** is not clearly understood as yet. Herein, we describe the synthesis and characterization of new rhodium and iridium species related to **2** which result from an unexpected bimetallic P_4-activation pathway.

Reaction of $[M(dppm)_2]OTf$ (M = Rh (**3**-OTf), Ir (**4**-OTf); dppm = $PPh_2CH_2PPh_2$, OTf = trifluoromethanesulfonate)[7] with white phosphorus in CH_2Cl_2 at room temperature under nitrogen and subsequent work up led to the isolation of $[M(dppm)(Ph_2PCH_2PPh_2PPPP)]OTf$ as either orange (M = Rh (**5**-OTf)) or light yellow (M = Ir (**6**-OTf), Scheme 1)

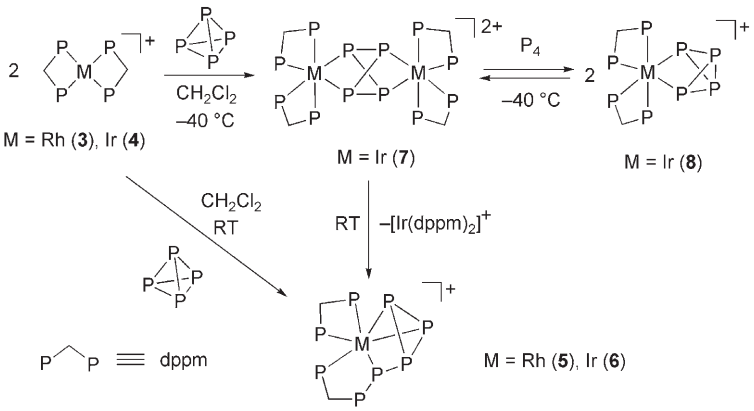

Scheme 1. Reactions of **3** and **4** with P_4. The Ph groups of the dppm ligands have been omitted.

microcrystals. Complexes **5**-OTf and **6**-OTf were characterized by ^1H and ^{31}P NMR spectroscopy, ESI mass spectrometry, elemental analysis, and single-crystal X-ray crystallography. The structure of the complex cation in **5**-OTf is presented in Figure 1 a,[8] and Figure 2 shows a plot of the experimental and computed $^{31}P\{^1H\}$ NMR spectra of **5**-PF_6 with the labeling scheme taken from the ORTEP drawing in Figure 1 a (NMR spectroscopic values for **5** and **6** are given in the Supplementary Information).

The structure of **5**-OTf consists of the $[Rh(dppm)(Ph_2PCH_2PPh_2PPPP)]^+$ cation and a triflate anion. In the complex cation, the metal is pseudo-octahedrally coordinated by a dppm ligand and by the new $Ph_2PCH_2PPh_2PPPP$ ligand, which originates from the attack of one terminal dppm Ph_2P group on the P_4 molecule. The whole activation process results in the cleavage of two P–P edges (P5–P7 and P5–P8) and subsequent attack on P5 by one dppm PPh_2 terminal group. Alternatively, the coordination polyhedron can be described as a trigonal bipyramid in which the P7–P8 bond occupies one site with an η^2-type coordination in the equatorial plane, and the P2-Rh1-P5 linkage forms the axis of the bipyramid. The bond lengths better represent the latter bonding picture, as the P7–P8 bond reveals the shortest P–P separation (2.118(3) Å) in the {PPPP} group, and the other P–P bonds (P6–P5, P6–P7, and P6–P8) average to 2.214(7) Å.[9] Notably, the latter value is practically unchanged in comparison with the average P–P

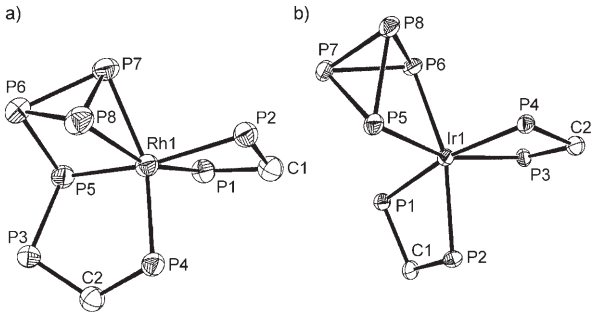

Figure 1. ORTEP drawings of the complex cations in **5**-OTf (a) and **8**-OTf (b); thermal ellipsoids are set at 30% probability. H atoms and phenyl groups are omitted. Selected bond lengths/separations [Å] and angles [°]: **5**-OTf: Rh1-P1 2.357(2), Rh1-P2 2.398(2), Rh1-P4 2.348(2), Rh1-P5 2.343(2), Rh1-P7 2.426(3), Rh1-P8 2.431(3), P3-P5 2.206(3), P5-P6 2.202(3), P6-P7 2.225(4), P6-P8 2.216(4), P7-P8 2.118(3), P5···P7 2.992(4), P5···P8 3.158(4); P1-Rh1-P8 159.60(9), P2-Rh1-P5 162.64(8), P4-Rh1-P7 153.29(9), P1-Rh1-P4 98.04(8), P1-Rh1-P7 108.20(9), P4-Rh1-P8 102.31(9), P7-Rh1-P8 51.71(9). **8**-OTf: Ir1-P1 2.349(2), Ir1-P2 2.435(2), Ir1-P3 2.418(2), Ir1-P4 2.327(2), Ir1-P5 2.411(2), Ir1-P6 2.430(2), P5-P7 2.231(3), P5-P8 2.237(3), P6-P7 2.233(3), P6-P8 2.214(3), P7-P8 2.162(3), P5···P6 2.760(3); P1-Ir1-P4 169.52(7), P3-Ir1-P5 159.52(7), P2-Ir1-P6 164.09(7).

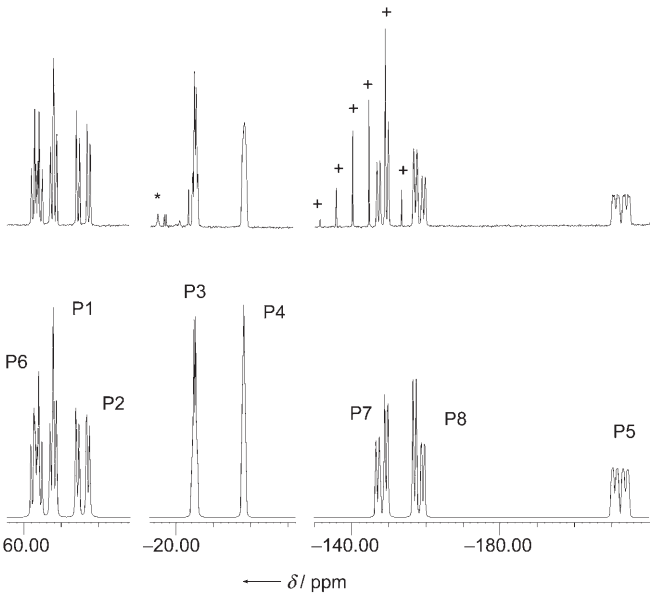

Figure 2. Computed (bottom) and experimental (top) $^{31}P\{^1H\}$ NMR spectra of **5**-PF_6 (400.13 MHz, CD_2Cl_2, 294 K); unidentified impurity denoted with ⋆; some of the signals of the partially superimposed PF_6 septet denoted with +.

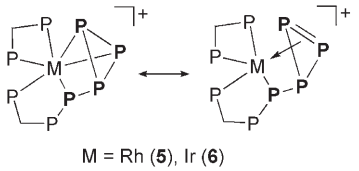

bond lengths determined for the free P_4 molecule (2.21 Å).[10] A similar bonding situation was found for the rhodium derivatives $[\{MeC(CH_2PPh_2)_3\}Rh(\eta^1{:}\eta^2\text{-}P_4RR')]^+$, which dis-

play metrical parameters and NMR data in agreement with a trigonal bipyramidal geometry.[11]

Compounds **5**-OTf and **6**-OTf are soluble in halogenated solvents, THF, and acetone. The $^{31}P\{^1H\}$ NMR spectra in CD_2Cl_2 indicate that the solid-state structures of **5** and **6** are preserved in solution. The spectrum of **5** exhibits a temperature-invariant ABCDEFGHX splitting pattern ($X = ^{103}Rh$), which simplifies to an ABCDEFGH pattern for the iridium complex **6** (see the Supporting Information).

Complexes **5** and **6** display a new P_4 topology formed by a *cyclo*-P_3 ring that is bound to a functionalized P atom;[12] this ligand array may be viewed as an intermediate along the P_4-activation process leading to the ligand in **2**. Indeed, further cleavage of the P6–P8 bond and subsequent attack on a PPh_2 group of a chelating dppm ligand could certainly account for the formation of the tetraphosphabutadiene unit $\{Ph_2PCH_2PPh_2PPPPPh_2PCH_2PPh_2\}$ that was found in the cobalt derivative **2**.[13] Monitoring the reactions of **3**-OTf and **4**-OTf with P_4 by in situ ^{31}P NMR spectroscopy provided useful hints about the activation mechanism. The strategy was to exploit the higher kinetic inertness of the Ir complex in the NMR monitoring of the reaction of **4**-OTf with P_4. White phosphorus immediately reacted with the iridium precursor already at −40 °C to afford a highly fluxional intermediate species **7** which displayed three featureless resonances at $\delta =$ −55.9, −62.1, and −82.6 ppm with identical intensity corresponding to four P atoms each. Lowering the temperature to −90 °C did not affect the broadness of these signals, thus indicating that a low-energy process is responsible for the observed fluxionality of **7**. Increasing the temperature to 25 °C slowly gave the final compound **6** in almost quantitative yield after about four days (Scheme 1). However, when the solution was kept at −40 °C, a new set of resonances appeared in the spectrum within 20 minutes, as ascribable to the Ir^{III} complex $[Ir(dppm)_2(\eta^2\text{-}P_4)]OTf$ (**8**-OTf) which results from the oxidative addition of P_4 to **7**-OTf. After a week at −20 °C, brown crystals of **8**-OTf precipitated.[14] The structure of **8**-OTf consists of a $[(dppm)_2Ir(\eta^2\text{-}P_4)]^+$ cation and a triflate anion, as well as a disordered dichloromethane molecule (Figure 1b). In **8**, the metal center is hexacoordinated by the four phosphorus donors of two dppm ligands and by an η^2-coordinated tetraphosphabicyclobutadienide ligand. The bond lengths in the P_4 moiety are comparable with those of other reported butterfly P_4 ligands.[2]

Dissolving **8**-OTf in CH_2Cl_2 did not directly produce **6**, but gave rise to an equilibrium between **8** and **7** with release of free P_4 (singlet at $\delta = -527$ ppm).[15] To elucidate the nature of **7**, stock solutions of **4**-OTf and P_4 in CD_2Cl_2 were carefully mixed at low temperature (−40 °C) in four screw-cap 5 mm NMR tubes to prepare solutions of **4**-OTf/P_4 in ratios of 1:0.25, 1:0.50, 1:1, and 1:2, and these solutions were independently analyzed by ^{31}P NMR spectroscopy at low temperature. The results of this experiment show that: 1) at the lowest P_4 concentration (1:0.25 **4**-OTf/P_4), only 50% of the iridium complex is consumed to form **7**, and the other signals correspond to unreacted **4**; 2) doubling the amount of P_4 (1:0.50 **4**-OTf/P_4) gives **7** as the only NMR-detectable iridium species, and all the added P_4 is consumed; and 3) further increase of P_4 concentration (1:1 or 1:2 **4**-OTf/P_4) does not change the product distribution and gives only free P_4 and **7**. As all experiments were performed quickly, no significant amount of **8** was detected. On this basis, we may conclude that the mononuclear species **8** is not directly related to the activation process and that a bimetallic complex of the form $[\{Ir(dppm)_2\}_2(\mu,\eta^2\text{:}\eta^2\text{-}P_4)]^{2+}$, which features a doubly activated tetraphosphorus molecule tethering two $\{Ir(dppm)_2\}$ fragments, is the most likely attribution for **7**. This conclusion is in line with literature data reporting double-edge activation of P_4 as observed in, for example, $[\{Cp^*Co(CO)\}_2(\mu,\eta^2\text{:}\eta^2\text{-}P_4)]$[4a] and $[\{HC(CMeNAr)_2\}_2Al_2(\mu,\eta^2\text{:}\eta^2\text{-}P_4)]$ (Ar = 2,6-*i*$Pr_2C_6H_3$),[4e] although species with $\mu,\eta^1\text{:}\eta^2\text{-}P_4$ or $\mu,\eta^1\text{:}\eta^1\text{-}P_4$ ligands, which could account for the observed fluxionality of **7** and for the formation of **6** by nucleophilic attack of one dppm PPh_2 group on the activated P_4 ligand, cannot be ruled out at this stage for the Ir complex. The occurrence of a bimetallic activation of white phosphorus by Mo^{III} complexes has been recently proposed.[16] Theoretical studies are in progress to clarify the nature of **7**, whose identification represents a step forward in understanding the activation of elemental phosphorus by transition metals and may eventually lead to large-scale applications. The reactivity of the novel complexes **5** and **6** is also currently under investigation.

In summary, we have shown that: 1) as in recent reports in N_2 chemistry,[17] bimetallic cooperativity is relevant to P_4 activation; 2) a new bonding mode for the P_4 ligand which catches the metal-mediated opening of the P_4 molecule in action has been elucidated; and 3) the ancillary phosphane ligands may actively participate in opening the P_4 cage, thus confirming that the activation/degradation of white phosphorus is favored by strong nucleophiles.[18]

Experimental Section

5-OTf: A solution of P_4 (0.030 g, 0.24 mmol) in THF (4 mL) was added to a solution of **3**-OTf (0.21 g, 0.19 mmol) in acetone (10 mL) at room temperature with continuous stirring. The resulting brown solution was concentrated under a current of nitrogen to about 5 mL, and then ethanol (10 mL) was added. After further concentration under nitrogen, allowing the solution to stand at room temperature for one day gave orange-brown X-ray quality crystals. The crystals were filtered, washed with acetone/pentane (1:1), and dried in a current of nitrogen at room temperature. Yield: 0.125 g, 58%. Elemental analysis (%) calcd for $C_{51}H_{44}F_3O_3P_8RhS$: C 53.51, H 3.87; found: C 53.38, H 3.97; ESI-MS: *m*/*z* (%): 995.4 (100) $[Rh(dppm)(Ph_2PCH_2PPh_2PPPP)]^+$; ^1H NMR (400.13 MHz, CD_2Cl_2, 294 K): $\delta = 8.4$–6.5 (m, 40H, Ph), 4.8–4.2 ppm (m, 4H, CH_2); $^{31}P\{^1H\}$ NMR: see Figure 2 and the Supporting Information. Metathesis of the triflate counteranion with NH_4PF_6 gave the PF_6 salt **5**-PF_6 in practically quantitative yield.

6-OTf: A solution of P_4 (0.026 g, 0.21 mmol) in THF (3 mL) was added to a solution of **4**-OTf (0.200 g, 0.17 mmol) in CH_2Cl_2 (15 mL) at room temperature. The resulting reddish-brown solution was stirred at room temperature until the color turned to orange-yellow (ca. 4 days). Then ethanol (10 mL) was added, and the solution was concentrated under a gentle current of nitrogen until precipitation started. After the solution stood for one day at room temperature, solid **6** separated as light yellow X-ray-quality crystals. The crystals were filtered, washed with CH_2Cl_2/pentane (1:3), and dried in a current of nitrogen. Yield: 0.110 g, 56%. Elemental analysis (%) calcd for $C_{51}H_{44}F_3IrO_3P_8S$: C 49.64, H 3.59; found: C 49.59, H 3.70; ^1H NMR (400.13 MHz, CD_2Cl_2, 294 K): $\delta = 7.6$–7.0 (m, 40H, Ph),

4.87 ppm (m, 4H, CH_2); $^{31}P\{^1H\}$ NMR: see the Supporting Information.

Details of the synthesis of **3**-OTf and **4**-OTf, as well as of the crystal-structure determination of **5**-OTf and **8**-OTf, are provided in the Supporting Information, which also includes complete ORTEP drawings of **5**-OTf and **8**-OTf, tables reporting the $^{31}P\{^1H\}$ NMR spectroscopic data for **5** and **6**, and copies of significant ^{31}P NMR spectra.

Received: March 16, 2006
Published online: May 16, 2006

Keywords: iridium · P ligands · phosphorus · rhodium · structure elucidation

[1] a) K. H. Whitmire, *Adv. Organomet. Chem.* **1998**, *42*, 1–145; b) O. J. Scherer, *Acc. Chem. Res.* **1999**, *32*, 751–762; c) M. Peruzzini, I. de los Rios, A. Romerosa, F. Vizza, *Eur. J. Inorg. Chem.* **2001**, 593–608; d) M. Ehses, A. Romerosa, M. Peruzzini, *Top. Curr. Chem.* **2002**, *120*, 107–140; e) M. Peruzzini, R. R. Abdreimova, Y. Budnikova, A. Romerosa, O. J. Scherer, H. Sitzmann, *J. Organomet. Chem.* **2004**, *689*, 4319–4331; f) M. Peruzzini, L. Gonsalvi, A. Romerosa, *Chem. Soc. Rev.* **2005**, *34*, 1038–1047.

[2] a) P. Dapporto, S. Midollini, L. Sacconi, *Angew. Chem.* **1979**, *91*, 510; *Angew. Chem. Int. Ed. Engl.* **1979**, *18*, 469–470; b) T. Gröer, G. Baum, M. Scheer, *Organometallics* **1998**, *17*, 5916–5919; c) M. Peruzzini, M. Marvelli, A. Romerosa, R. Rossi, F. Vizza, F. Zanobini, *Eur. J. Inorg. Chem.* **1999**, 931–933; d) I. de los Rios, J. R. Hamon, P. Hamon, C. Lapinte, L. Toupet, A. Romerosa, M. Peruzzini, *Angew. Chem.* **2001**, *113*, 4028–4030; *Angew. Chem. Int. Ed.* **2001**, *40*, 3910–3911; e) M. Di Vaira, S. Seniori Costantini, P. Stoppioni, P. Frediani, M. Peruzzini, *Dalton Trans.* **2005**, 2234–2236.

[3] M. Di Vaira, S. Seniori Costantini, P. Stoppioni, P. Frediani, M. Peruzzini, Book of abstracts, XXth IUCR Congress, Florence, Italy, **2005**, C303-P.07.01.37.

[4] a) O. J. Scherer, M. Swarowsky, H. Swarowsky, G. Wolmershäuser, *Angew. Chem.* **1988**, *100*, 738–739; *Angew. Chem. Int. Ed. Engl.* **1988**, *27*, 694–695; b) O. J. Scherer, M. Swarowsky, H. Swarowsky, G. Wolmershäuser, *Organometallics* **1989**, *8*, 841–842; c) O. J. Scherer, G. Schwarz, G. Wolmershäuser, *Z. Anorg. Allg. Chem.* **1996**, *622*, 951–957; d) V. A. Miluykov, O. G. Sinyashin, P. Lönnecke, E. Hey-Hawkins, *Mendeleev Commun.* **2003**, 212–213; e) Y. Peng, H. Fan, H. Zhu, H. W. Roesky, J. Magull, C. E. Hughes, *Angew. Chem.* **2004**, *116*, 3525–3527; *Angew. Chem. Int. Ed.* **2004**, *43*, 3443–3445.

[5] a) E. Hey, M. F. Lappert, J. L. Atwood, S. G. Bott, *J. Chem. Soc. Chem. Commun.* **1987**, 597–598; b) P. J. Chirik, J. A. Pool, E. Lobkovsky, *Angew. Chem.* **2002**, *114*, 3613–3615; *Angew. Chem. Int. Ed.* **2002**, *41*, 3463–3465; c) A. R. Fox, R. J. Wright, E. Rivard, P. P. Power, *Angew. Chem.* **2005**, *117*, 7907–7911; *Angew. Chem. Int. Ed.* **2005**, *44*, 7729–7733.

[6] a) F. Cecconi, C. A. Ghilardi, S. Midollini, A. Orlandini, *J. Am. Chem. Soc.* **1984**, *106*, 3667–3668; b) F. Cecconi, C. A. Ghilardi, S. Midollini, A. Orlandini, *Inorg. Chem.* **1986**, *25*, 1766–1770.

[7] The preparations of **3**-OTf and **4**-OTf are detailed in the Supporting Information.

[8] Crystal data for **5**-OTf: $C_{51}H_{44}F_3O_3P_8RhS$, $M_r = 1144.59$, triclinic, space group $P\bar{1}$, $a = 19.755(6)$, $b = 12.139(3)$, $c = 11.744(3)$ Å, $\alpha = 73.75(2)$, $\beta = 108.20(2)$, $\gamma = 102.55(2)°$, $V = 2542(1)$ Å^3, $Z = 2$, $\rho_{calcd} = 1.495$ Mg m^{-3}, $\mu(Cu_{K\alpha}) = 5.926$ mm^{-1}, $F(000) = 1164$. A total of 4103 reflections were collected at room temperature on a Philips PW 1100 automatic diffractometer with $Cu_{K\alpha}$ radiation. The structure was solved by direct methods and refined by full-matrix F^2. The phenyl rings were treated as rigid bodies, and anisotropic temperature factors were assigned only to non-hydrogen and non-carbon atoms to ensure a good parameter-to-data ratio. Some constraints were applied to the disordered triflate anion. The hydrogen atoms were introduced in calculated positions with thermal factors 20% larger than those of the corresponding carbon atoms. $R_1 = 0.0584$ and $wR_2 = 0.1478$ for 3610 reflections ($I > 2\sigma(I)$). CCDC-299453 contains the supplementary crystallographic data for **5**-OTf. These data can be obtained free of charge from The Cambridge Crystallographic Data Centre via www.ccdc.cam.ac.uk/data_request/cif.

[9] A similar structure has been ascertained by X-ray crystallography for the isomorphous iridium complex **6**-OTf: triclinic, space group $P\bar{1}$, $a = 19.822(10)$, $b = 12.113(6)$, $c = 11.820(6)$ Å, $\alpha = 73.47(6)$, $\beta = 108.26(9)$, $\gamma = 103.14(9)°$; A. Orlandini et al., unpublished results.

[10] Chemical Society Special Publication No. 18, Chemical Society, London, **1965**.

[11] P. Barbaro, A. Ienco, C. Mealli, M. Peruzzini, O. J. Scherer, G. Schmitt, F. Vizza, G. Wolmershäuser, *Chem. Eur. J.* **2003**, *9*, 5195–5210.

[12] The zirconium complex $[Cp_2Zr\{\eta^1{:}\eta^1\text{-}P_4(PR_2)_2\}]$ shows a correlated structural motif in which the tetraphosphorus ligand is part of a P_6 moiety which incorporates two phosphido units originally coordinated to zirconium.[5a]

[13] The thermal lability of **5** and **6** does not allow to verify directly this mechanistic proposal. Studies on the corresponding dppm–Co system are in progress to confirm this hypothesis.

[14] $[Ir(dppm)_2(\eta^2\text{-}P_4)]OTf{\cdot}0.5\,CH_2Cl_2$ (**8**-OTf·0.5 CH_2Cl_2): $^{31}P\{^1H\}$ NMR (81.015 MHz, CD_2Cl_2, 233 K): $\delta = -51.5$ (m, 2P, dppm), −81.30 (m, 2P, dppm) −236.90 (m, 2P, P_4), −250.80 ppm (m, 2P, P_4). Crystal data for **8**-OTf·0.5 CH_2Cl_2: $C_{51.5}H_{45}ClF_3IrO_3P_8S$, $M_r = 1276.34$, monoclinic, space group $P2_1/c$, $a = 14.126(9)$, $b = 17.032(9)$, $c = 25.226(8)$ Å, $\beta = 102.22(2)°$, $V = 5932(5)$ Å^3, $Z = 4$, $\rho_{calcd} = 1.429$ Mg m^{-3}, $\mu(Mo_{K\alpha}) = 2.594$ mm^{-1}, $F(000) = 2540$. A total of 10391 reflections were collected on an Oxford CCD automatic diffractometer with $Mo_{K\alpha}$ radiation at 190 K. The structure was solved by direct methods and refined by full-matrix F^2. All the non-hydrogen atoms, except for those of the disordered solvent molecule, were assigned anisotropic temperature factors. The phenyl rings were refined as rigid groups of D_{6h} symmetry. The hydrogen atoms were introduced in calculated positions with temperature factors 20% larger than those of the respective carbon atoms. $R_1 = 0.0677$ and $wR_2 = 0.1682$ for 8757 reflections ($I > 2\sigma(I)$). CCDC-604167 contains the supplementary crystallographic data for **8**-OTf·0.5 CH_2Cl_2. These data can be obtained free of charge from The Cambridge Crystallographic Data Centre via www.ccdc.cam.ac.uk/data_request/cif.

[15] In situ NMR studies on the rhodium precursor **3**-OTf and P_4 did not give the analogue of **8**, but confirmed that the formation of **5** is preceded by the formation of a fluxional three-band species similar to **7** ($^{31}P\{^1H\}$ NMR: $\delta = -13.02$ (br d, $^1J_{RhP}$ 95 Hz), −51.98 (br d $^1J_{RhP}$ 76 Hz), −59.84 ppm (br s)). For the Rh system, the concentration of this intermediate does not grow substantially at any temperature in the ^{31}P NMR spectrum as it transforms into **5** at a much faster rate than **7** transformed into **6** (ca. 1 hour at −40 °C; immediately at room temperature).

[16] F. H. Stephens, M. J. A. Johnson, C. C. Cummins, O. P. Kryatova, S. V. Kryatov, E. V. Rybak-Akimova, J. E. McDonough, C. D. Hoff, *J. Am. Chem. Soc.* **2005**, *127*, 15191–15200.

[17] F. Studt, B. A. MacKay, S. A. Johnson, B. O. Patrick, M. D. Fryzuk, F. Tuczek, *Chem. Eur. J.* **2005**, *11*, 604–608, and references therein.

[18] a) A. Schmidpeter, S. Lochshmidt, S. Sheldrick, *Angew. Chem.* **1985**, *97*, 214–215; *Angew. Chem. Int. Ed. Engl.* **1985**, *24*, 226–227, and references therein; b) J. P. Bezombes, P. B. Hitchcock, M. Lappert, J. E. Nycs, *Dalton Trans.* **2004**, 499–501.

